ICANS-XIV
14th Meeting of the International Collaboration on Advanced Neutron Sources
Starved Rock Lodge, Utica Ill., USA
June 14-19, 1998

Neutronic Aspects of the SINQ Mark 2 Target with Irradiation Test Samples

A. Dementyev *), G.S. Bauer, Y. Dai and E. Lehmann
*) Guest from Institute for Nuclear Research Moscow, Russia

Paul Scherrer Institut, CH-5232 Villigen-PSI, Switzerland

Abstract

The radiation fields and power deposition levels in a heavy water cooled Zircaloy rod target for SINQ are examined, with particular attention to so called "experimental rods" which contain miniature radiation effects test samples of steel between filler pieces in Zircaloy tubes. Because the geometric model is a very detailed one, we were able to analyse individual rods in their discrete environment. As result, the radiation environment and the power distribution in the different target versions could be compared in detail. Furthermore, some results for rod bundles containing Lead in Aluminium cladding are reported.

1. Introduction

The target for the commissioning phase of the continuous spallation neutron source SINQ consists of Zircaloy-2 rods which are arranged perpendicular to the proton beam. This array is welded into the hexagonal target case and is cooled by heavy water (to avoid neutron losses by absorption which would occur if light water is used). This target concept was chosen for its simplicity and because very limited information was available on the behaviour of materials under irradiation in a spallation source radiation field. With Zircaloy, a proven reactor material, the most serious worry is embrittlement due to formation of hydride.

Since, according to calculations [1], the neutron yield of this target is by a factor of 2-2.5 lower than what could be achieved by an optimally designed target on the basis of Lead as spallation material, there is a strong incentive to change to a different target concept.

For this transition, and also for future spallation sources like ESS [2] it is very important to know the effects of irradiation on structural materials in order to be able to assess the life expectancy and operational safety of the target. There are some favourite alloys for use as cladding material

Keywords: SINQ Target, Rod Target, Neutronic Performance, Radiation Fields, Power deposition

for Lead or as containers for liquid metals, but knowledge on their behaviour under high level irradiation is very limited, because there are doubts whether the results from reactor irradiation are valid due to the much higher gas production (He and H) in a spallation environment

Therefore, it was decided to launch a materials programme at PSI [3]. As part of this programme several of the standard Zircaloy rods along the beam axis are replaced by experimental rods in the second target for SINQ which will be used from July 1998 on. These experimental rods have a Zircaloy cladding and contain a large number of miniature samples of the material to be investigated which are embedded between filling material of Aluminium or Zircaloy. The 1500 micro samples have dimensions from 3 to 24 mm [4]. Fig. 1 illustrates how the 10 rods are positioned in the rod bundle matrix. It also shows some more special target elements on off-axis positions which are either solid steel or prototypes of steel clad lead rods.

Because the experimental rods represent a deviation from the licensed standard target and in order to estimate the thermal, stress and flux conditions under which the specimens would be irradiated, a thorough assessment of the nuclear and mechanical loads in the new target was necessary. In this paper we report on the nuclear and neutronic part of the work; the mechanical aspects, for which these results served as a basis are reported elsewhere [5].

2. Calculational modelling

Using a rather detailed geometric model [6] which represents the rods and tubes in the target individually and part of which is shown in Fig. 2, the power deposition and flux distribution in the target were studied. The intensity in the incident proton has been given [7] as being of elliptic cross section with a truncated Gaussian distribution:

$$i(r) = I_0/(2\pi ab)*\exp(-1/2[(x/a)^2+(y/b)^2]) / [1-\exp(-c^2/2)], \quad (1)$$

where a and b are the standard deviations of the Gaussian distributions in x and y and the cut-off is given by the condition

$$(x/a)^2 + (y/b)^2 \leq c^2. \quad (2)$$

To a first approximation the beam can be described as having the form of a Gaussian with radial symmetry and a standard deviation $a = b = \sigma$ of 3.7 cm. Taking $c = 2$, the intensity distribution can be represented with $r^2=x^2+y^2$ as:

$$i(r) = I_0*/(2\pi\sigma^2)*\exp(-r^2/2\sigma^2)/ [1- e^{-2}], \quad (3)$$

This relation describes the one given in [7] fairly well and was used in the present calculations.

Whereas the heat deposition can be calculated by the high energy code LAHET [8] alone, the coupled MCNP code must be used to determine the thermal flux distribution around the target region, which is much more time consuming.

The modified rods where described as homogeneous mixtures of the materials contained in them. Three cases were considered:

- a mixture of aluminium and iron in the Zircaloy tube as replacement for the Zircaloy rods
- substitution of additional four rods by stainless steel as shown in Fig. 1.
- Lead rods with aluminium as cladding material.

3. Spectral and flux conditions in the target region

3.1 Proton energy and flux

As the proton beam penetrated into the target its average energy and intensity decrease, while its energy spread at each position increases. Knowledge of theses spectral details is important for the final evaluation of the radiation damage measured in the post irradiation examination of the test specimens. The change of intensity and spectral composition of the proton beam was, therefore, examined at the position of each one of the experimental rods. The results, averaged over a length of 2 cm around the middle of each rod, are shown in Fig 3 with the proton energy as independent variable and the rod number as parameter. Rod # 1 is the rod closest to the beam window. The total proton flux at each position is the integral under the respective curve.

In order to estimate the power distribution along the rods as the beam widens while it penetrates into the target, each rod was subdivided into 9 segments and the total number of protons hitting each segment was counted. The results are shown in Fig 4 in units of total proton flux per mA beam. It may be assumed that, to a first approximation, the spectral distribution remains unchanged over the length of the rod.

Clearly, as the beam penetrates into the target it widens and the intensity distribution along the rods becomes flatter. The peak values of the neutron flux for all experimental rods will be shown together with the neutron fluxes in the next section.

3.2 Neutron spectra and intensities

The neutron spectrum in the energy range between about 1meV up to 1 MeV shows little variation for the positions of the different rods. (Fig. 5). As for the thermal part of the spectrum no significant variation would be expected due to the long transport length of a heavy water moderated and reflected system with low absorption in the target region.

Also, since cascade neutrons are preferentially emitted in the forward direction, less variation is observed in the high energy neutron flux (above 20 MeV) than in the proton flux, as can be seen from Fig. 6.

For the radiation damage generated in the material the proton flux as well as the neutron flux above 0.1 to 0.5 MeV play the dominant role. In Figs 7 and 8 we compare the peak values of the proton flux at the positions of the experimental rods to the neutron flux above 0.1 and 0.5 MeV respectively. It is obvious that a large contribution comes from neutrons between the two energies.

4. Power dissipation in the target region

Since it is very time consuming to compute in detail the power dissipation in each rod as a function of position, this was done for one case only and all the following comparisons were made for the average power in individual rods only. Fig. 9 shows the power density calculated for the first Zircaloy rod in the target in comparison to the mean value obtained from an independent calculation. It can be seen that, in Zircaloy, the power dissipation is almost completely determined by the proton beam distribution. In cases where absorption of longer range secondary particles play a more dominant role, the peak-to-average ratio will be lower than that of the proton beam and therefore, using the distributions given in Fig 4 will always yield a peak power distribution that is on the safe side when used for temperature and stress calculations.

The average power densities in the experimental rods for the cases where Aluminium or Zircaloy is used as filler material is shown in Fig 10 in comparison to the case, of pure Zircaloy rods. The irregular behaviour stems from the fact that the steel content varies from one rod to the next. Fig. 10 shows that, by adding the steel samples to the rods, some 5% increase of average power density is generated, if Zircaloy is used as filler material, but can even be made lower than in pure Zircaloy by using Aluminium as filler material. The case of the massive steel rods was also examined and it was found that the power density in this case is increased by 30% over Zircaloy.

Finally the power dissipation in all target rods was examined for the case of lead filled Aluminium rods relative to Zircaloy and Lead rods only. This complements earlier work [9] and allows to compare the results obtained from using different code systems. In the case of Lead in the target its higher stopping power for protons plays an important role. Fig. 11 shows the average power density in the individual rods as a function of their layer number (position along the proton beam). It can be seen that, at the proton energy of 570 MeV available at SINQ, a Bragg peak still exists at the end of the range but is rather smeared out and not very intense.

It can be seen from Fig. 11 that, while about 46 layers of rods are required to range out the protons completely for Zircaloy, 40 will be enough for the case of lead filled aluminium tubes.

5. Neutron flux in the moderator

Clearly, introducing a small amount of steel and aluminium into 1o out of 450 target rods would not be expected to result in any significant changes in the flux or spectral distribution in the D_2O moderator surrounding the target. However, since it could be done conveniently, the neutron spectra were sampled at a point 20 cm from the target axis and 15 cm above the centre of the hemispherical bottom end of the target shell (i.e. the lower ege of the rod bundle (cf Fig 1). The results are shown for the whole energy range from 1 meV to 10 MeV in Fig 12 and for the thermal regime alone in Fig. 13. As expected, the differences are barely discernible and no adverse effects will be seen by the users due to the experimental rods in the target.

6. Conclusions

The analysis presented in this paper shows that introducing the experimental rods in the SINQ target Mark 2 will not affect the neutron flux in the reflector of SINQ but the radiation levels in the target and their spatial and spectral distributions will be suitable for the planned investigations on the test samples. Expected power densities were determined and can be used to examine the thermo-mechanical situation in the test rods in detail. Results of this work will be reported elsewhere. Using Aluminium as a filler material for the experimental rods will result in a total power per rod which is lower than for pure Zircaloy, but even for Zircaloy fillers the heat flux on the rod surfaces will be very moderate.

References:

[1] G.S. Bauer, A. Dementyev , E. Lehmann "Target Options for SINQ - A Neutronic Assessment" this conference

[2] ESS-Final Report, G.S. Bauer, T. Broome, D. Filges, H. Jones, H. Lengeler, A. Letchford, G. Rees, H. Stechemesser and G. Thomas, eds. "ESS, a Next Generation Neutron Source for Europe ", Vol III, The Ess Technical Study, ESS 96-53-M (1996),ISBN 90 237 6 659

[3] G.S. Bauer, Spallation neutron source material research at SINQ, Research proposal dated 21.10.1996

[4] G.S. Bauer, Y. Dai and L. Ni "Experience and Research on Target and structural Materials at PSI", submitted to Proc Int. Workshop on JHF Science, KEK, Tsukuba, Japan and PSI-report 98-04 (1998)

[5] L. Ni, and G.S. Bauer, "Thermal Structure Analyses on the Test Rods in the SINQ target Mark 2" this conference

[6] D. Dementyev, E. Lehmann, and G.S. Bauer "Computational Modelling and Assessment of SINQ with Zircaloy Target by the Code System LAHET" internal report PSI TM-36-97-02 (1998)

[7] U. Rohrer "Protonenstrahl für die SINQ" internal report SINQ/851/RU13-001.-

[8] R. Prael, H. Lichtenstein, User Guide to LCS: The LAHET Code system, LA-UR-89-3014

[9] F. Atchison, Operational Parameters for the Canneloni-Target, TM-816/AF30-303

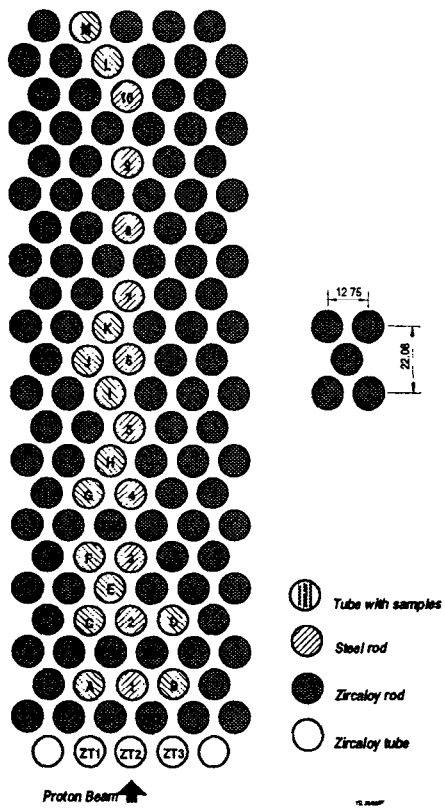

Fig. 1: Vertical section through the lower part of the modified zircaloy rod bundle equipped for investigations of the irradiation behaviour of structural material samples

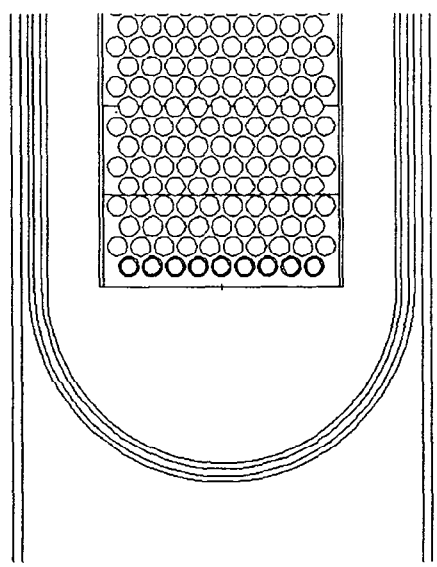

Fig. 2: Part of the model for the target of SINQ accounting each individual rod

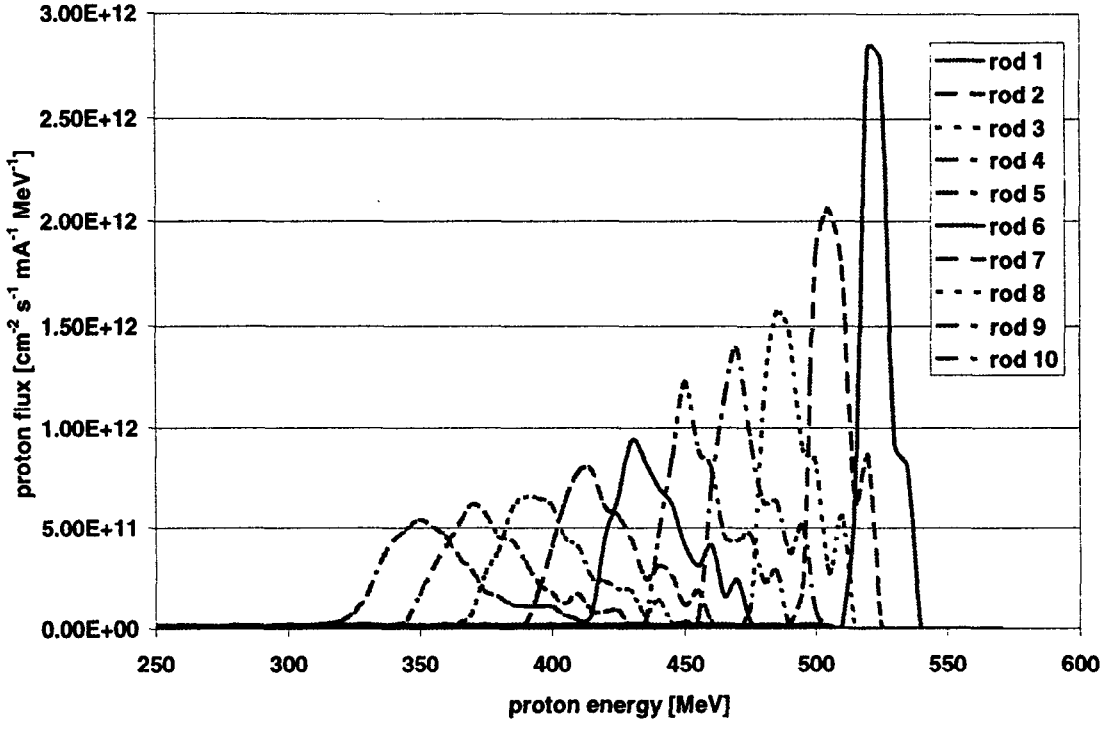

Fig 3: Proton flux spectra in the individual rods (cf Fig. 1) in the centre line of the modified Zircaloy target, averaged over the middle 2 cm of each rod

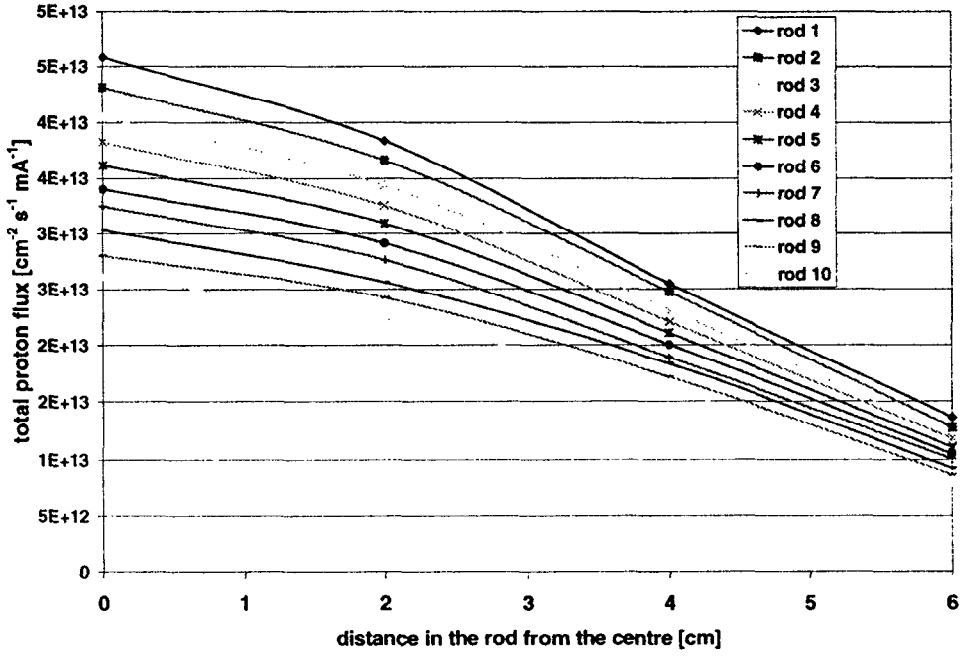

Fig. 4: Proton flux in the 10 experimental rods as a function of position along the rods.

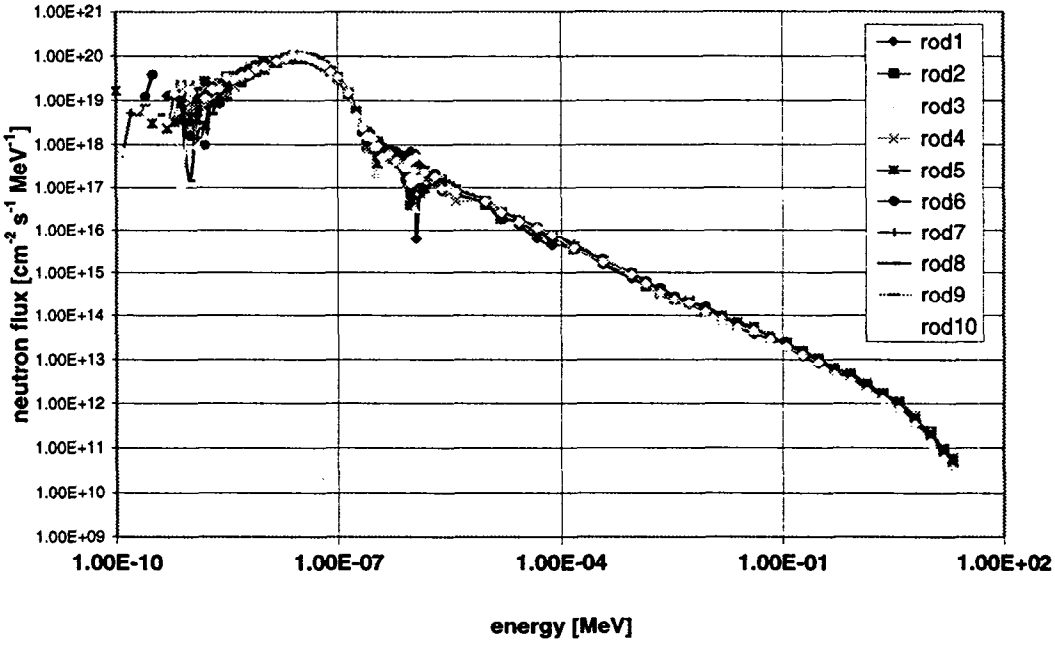

Fig. 5: Neutron spectra at the 10 modified rods of the zircaloy rod bundle target

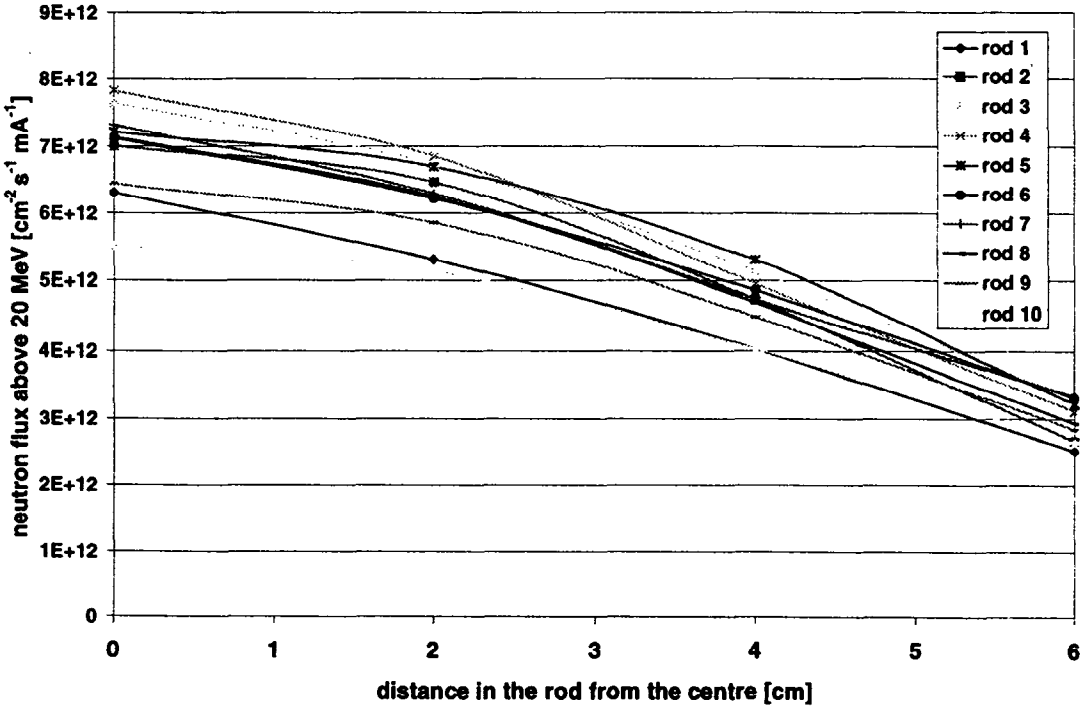

Fig. 6: Distribution of the high energy flux (above 20 MeV) along the 10 expeimental rods

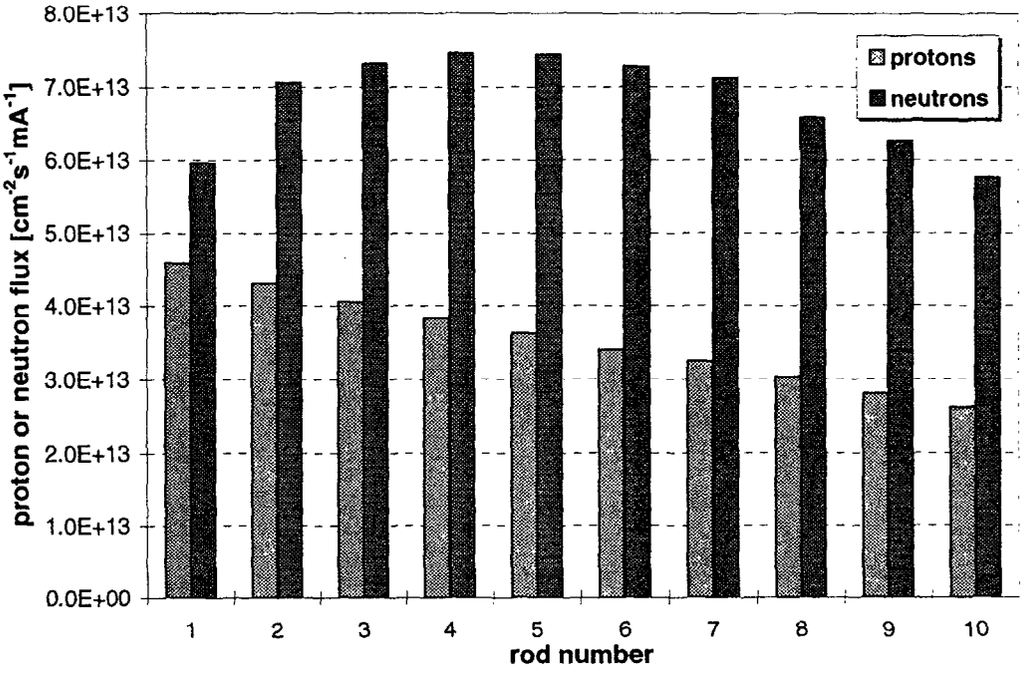

Fig. 7: Maximum proton and neutron flux (above 0.1 MeV) at the positions of the experimental rods

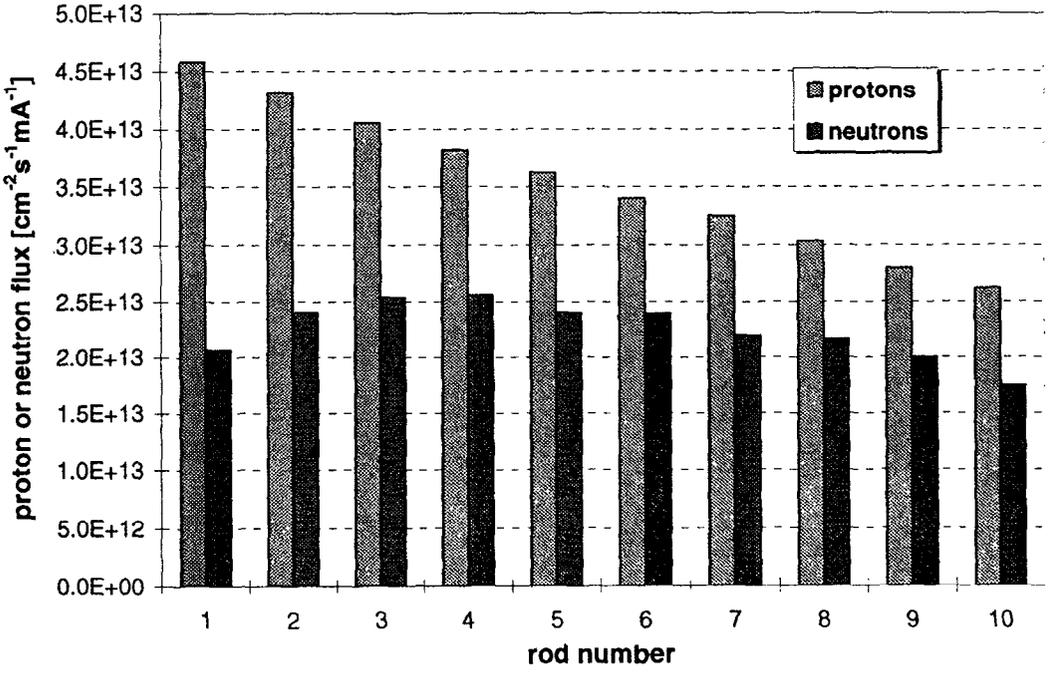

Fig. 8: Maximum proton and neutron flux (above 0.5 MeV) at the positions of the experimental rods.

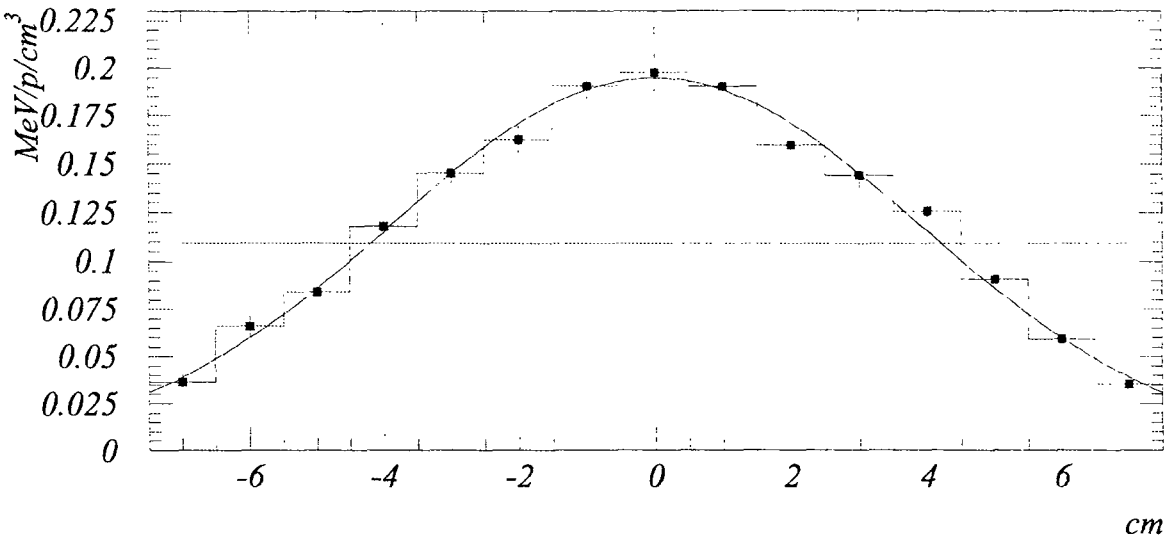

Fig. 9: Power density along the rod in the first line of the Zircaloy target compared to the average value of this rod

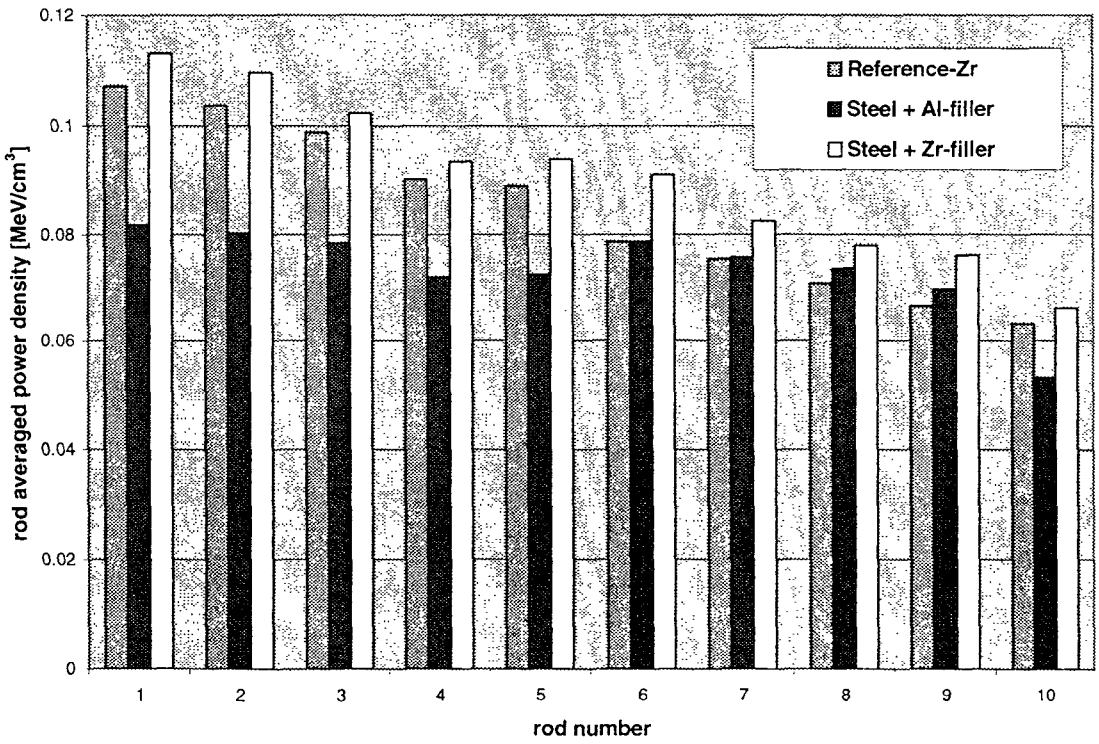

Fig. 10: Average power densities of the experimental target rods in the central plane (see Fig.1) in comparison to the Zircaloy rods

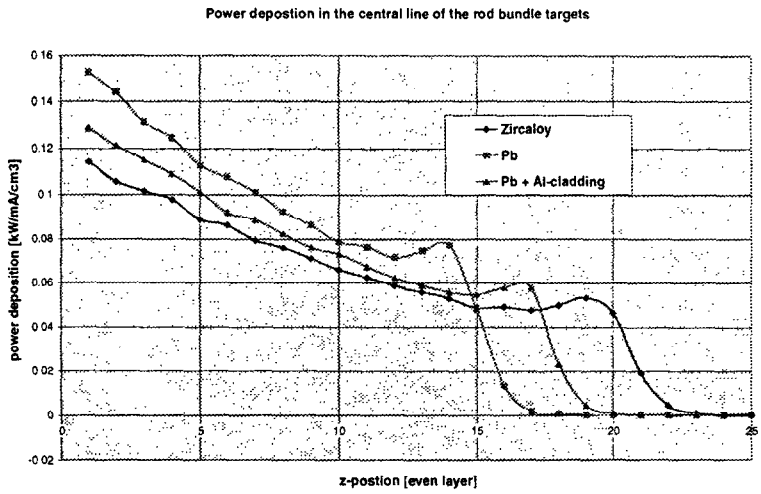

Fig. 11: Average power density in the target rods located in the central plane for different rod bundle targets for different target materials

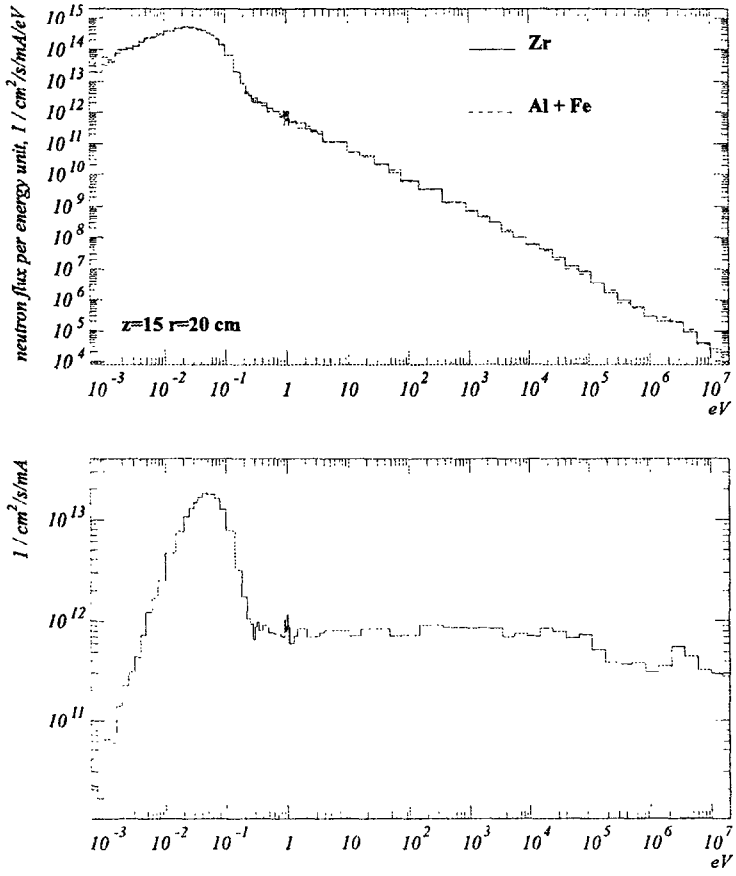

Fig. 12: Neutron spectra inside the moderator tank at the position r = 20 cm z =15 cm for the Zircaloy rod targets with and without the experimental rods. No visible difference is found. (Top: spectrum per neutron energy, below: lethargy representation).